Controlled analysis of nanoparticle charge on mucosal and systemic antibody responses following pulmonary immunization

Catherine A. Fromen[a,1], Gregory R. Robbins[b,c,1], Tammy W. Shen[d], Marc P. Kai[a], Jenny P. Y. Ting[b,c,2,3], and Joseph M. DeSimone[a,b,d,e,2,3]

[a]Department of Chemical and Biomolecular Engineering, North Carolina State University, Raleigh, NC 27695; and [b]Lineberger Comprehensive Cancer Center, Departments of [c]Microbiology-Immunology and [e]Chemistry, and [d]Eshelman School of Pharmacy, University of North Carolina at Chapel Hill, Chapel Hill, NC 27599

Contributed by Joseph M. DeSimone, December 2, 2014 (sent for review September 16, 2014; reviewed by Yong-Jun Liu and Chad A. Mirkin)

Pulmonary immunization enhances local humoral and cell-mediated mucosal protection, which are critical for vaccination against lung-specific pathogens such as influenza or tuberculosis. A variety of nanoparticle (NP) formulations have been tested preclinically for pulmonary vaccine development, yet the role of NP surface charge on downstream immune responses remains poorly understood. We used the Particle Replication in Non-Wetting Templates (PRINT) process to synthesize hydrogel NPs that varied only in surface charge and otherwise maintained constant size, shape, and antigen loading. Pulmonary immunization with ovalbumin (OVA)-conjugated cationic NPs led to enhanced systemic and lung antibody titers compared with anionic NPs. Increased antibody production correlated with robust germinal center B-cell expansion and increased activated CD4$^+$ T-cell populations in lung draining lymph nodes. Ex vivo treatment of dendritic cells (DCs) with OVA-conjugated cationic NPs induced robust antigen-specific T-cell proliferation with ∼100-fold more potency than soluble OVA alone. Enhanced T-cell expansion correlated with increased expression of surface MHCII, T-cell coactivating receptors, and key cytokines/chemokine expression by DCs treated with cationic NPs, which were not observed with anionic NPs or soluble OVA. Together, these studies highlight the importance of NP surface charge when designing pulmonary vaccines, and our findings support the notion that cationic NP platforms engender potent humoral and mucosal immune responses.

vaccine | cationic | nanoparticle | pulmonary | mucosal

The lung is a primary site of pathogen entry and is therefore a critical target for mucosal vaccination. Conventionally administered vaccines (e.g., s.c. or intramuscular injection) provide strong humoral protection, but often fail to generate mucosal immunity, especially in the form of IgA (1). Mucosal vaccines not only provide local protection, but also confer systemic immunity, including distal mucosal sites (1–3). Mucosal and systemic antibody responses require complex cross-talk between innate and adaptive immune cells. Antigens are first encountered by professional antigen presenting cells (APCs), such as dendritic cells (DCs), at the site of infection or injury. Activated DCs migrate to the draining lymph node (dLN), where they present antigenic peptides on MHCII, which allows for activation of antigen-specific CD4$^+$ T cells. Activated T cells instruct antigen-specific B cells to form germinal centers (GC) in the dLN where B cells expand, undergo affinity maturation, and Ig class switch recombination, resulting in production of highly specific antibodies with specialized functions (4). All three cell types (DCs, CD4$^+$ T cells, and B cells) are required for GC formation, because T-cell–deficient mice fail to form GCs and DC depleted mice exhibit reduced antibody production (5–7).

Nanoparticle (NP) formulations are being engineered to improve subunit vaccine approaches that induce pathogen mimicry while still maintaining the safety of subunit vaccines (8, 9). In the lung, NP formulations offer potential solutions to overcome biological barriers and target APCs (2, 10–13). Cationic NP formulations have been shown to increase mucosal antibody production following pulmonary or intranasal administration (14, 15), whereas independent studies using anionic NP approaches show only minimal improvement in antibody production compared with immunization with soluble protein alone (16, 17). To date, no direct evaluation of NP surface charge on mucosal immune responses has been performed, likely due to limitations in NP formulation that prevent such a comparison without dramatically changing NP composition. Our studies used the unique Particle Replication in Non-Wetting Template (PRINT) process to exquisitely control all other nanoparticle characteristics and specifically investigate the role of NP charge on vaccine responses.

Results

Cationic and Anionic NPs Synthesized Using the PRINT Process Can Be Reproducibly Functionalized with Ovalbumin. To specifically determine the role of surface charge on NP-based vaccines, we used a water soluble conjugation scheme to functionalize PRINT NPs that allows reproducible control over both protein loading and charge (zeta potential). The PRINT-fabricated hydrogel NPs used in these studies were inherently cationic [referred to as

Significance

To our knowledge, no other nano-based vaccine delivery platform has directly assessed the effects of nanoparticle charge on pulmonary vaccination without affecting other physio/chemical particle characteristics and/or antigen loading. The Particle Replication in Non-Wetting Templates nanoparticle fabrication process is unique in that it allows for isolation of charge as the sole variable in these studies while maintaining all other physical and chemical parameters constant. We find that positively charged nanoparticles induce robust mucosal and systemic antibody responses following pulmonary administration, whereas negatively charged nanoparticles fail to do so. Therefore, our studies underscore the importance of considering nanoparticle charge as a critical design parameter when generating pulmonary-based vaccines and may have implications for particulate vaccination through other routes of administration.

Author contributions: C.A.F., G.R.R., T.W.S., M.P.K., J.P.Y.T., and J.M.D. designed research; C.A.F., G.R.R., T.W.S., and M.P.K. performed research; C.A.F., G.R.R., T.W.S., and M.P.K. contributed new reagents/analytic tools; C.A.F. and G.R.R. analyzed data; and C.A.F., G.R.R., J.P.Y.T., and J.M.D. wrote the paper.

Reviewers: Y.-J.L., MedImmune; and C.A.M., Northwestern University.

Conflict of interest statement: J.M.D. is a founder and maintains financial interest in Liquidia Technologies.

[1]C.A.F. and G.R.R. contributed equally to this work.

[2]J.P.Y.T. and J.M.D. contributed equally to this work.

[3]To whom correspondence may be addressed. Email: desimone@unc.edu or jenny_ting@med.unc.edu.

This article contains supporting information online at www.pnas.org/lookup/suppl/doi:10.1073/pnas.1422923112/-/DCSupplemental.

(ζ^+)NPs], due to amine-functional groups incorporated into the NP matrix. Anionic NP [referred to as (ζ^-)NP] were generated by converting the amine groups on (ζ^+)NP to terminal carboxylate groups by using succinic anhydride, yielding a net negative charge. By using the same initial batch for positively and negatively charged NPs, we were able to control for all other NP characteristics (size, shape, composition) and isolate charge as the single variable in these studies. A model antigen, ovalbumin (OVA), was covalently bound through an amide bond to (ζ^+)NPs through the reaction in Fig. 1*A*. (ζ^-)NPs were covalently bound to OVA in a similar fashion following the succinylation reaction to yield a negative charge (Fig. 1*B*). OVA was covalently conjugated at 100 ± 10 μg of OVA/mg of NP ($n \geq 5$) on both cationic and anionic NPs, with unreacted amine or carboxylic groups maintaining the overall net charge. NPs remained monodisperse following OVA loading as measured by dynamic light scattering (DLS) analysis (Table S1) and scanning EM (Fig. 1*C*). Hydrodynamic diameters (Z_{avg}) and low polydispersity index (PDI) were consistent for all four particle formulations with a slight increase in Z_{avg} upon functionalization, likely due to OVA conjugation (Table S1). Minor variation in the Z_{avg} was observed overall between cationic and anionic formulations, amounting to slight differences in hydrogel swelling in the particular aqueous conditions of the DLS measurements and the general error associated with assigning a spherical diameter to a nonspherical NP (Table S1). However, extensive scanning EM measurements ensure fidelity between both (ζ^+)NP-OVA and (ζ^-)NP-OVA in all three dimensions. These results indicate that an equivalent amount of OVA was conjugated to both cationic and anionic PRINT NPs and did not induce particle aggregation.

DCs Treated with Particulate OVA Induce Robust OT-II CD4$^+$ T-Cell Proliferation ex Vivo. To determine how NP charge affects cellular uptake, antigen processing, and presentation by MHCII, we treated bone marrow-derived dendritic cells (BMDCs) (gating and purity in Fig. S1 *A* and *B*) with (ζ^+)NP-OVA or (ζ^-)NP-OVA and tested their ability to induce antigen-specific T-cell proliferation by using CFSE-labeled OVA-specific CD4$^+$ T cells from transgenic OT-II mice (purity in Fig. S1*C*). BMDCs treated with soluble OVA induced T-cell proliferation in a dose-dependent manner with a 10 μg/mL dose, resulting in ∼77% of antigen-specific T cells undergoing >3 divisions (Fig. 1*D, Upper*, full gating in Fig. S1*D*). Both (ζ^-)NP-OVA and (ζ^+)NP-OVA induced similar responses by using 10-fold lower OVA concentrations than soluble controls (Fig. 1*D, Middle* and *Lower*, respectively). T-cell proliferation in response to (ζ^+)NP-OVA–treated DCs was even stronger at 0.1 μg/mL OVA dose, whereas the response to (ζ^-)NP-OVA–treated DCs declined precipitously and was undetectable with soluble OVA (Fig. 1*D*). At the 0.01 μg/mL dose, the (ζ^+)NP-OVA–treated DC induced ∼28% of T cells to undergo >3 divisions with undetectable proliferation in response to (ζ^-)NP-OVA and soluble OVA-treated DCs (Fig. 1*D*). The ability of DCs treated with (ζ^+)NP-OVA to induce robust T-cell proliferation was highly reproducible, because similar results were observed with multiple batches of independently synthesized NP-OVA and cell preparations (Fig. 1*E*). From these data, we conclude that DCs treated with (ζ^+)NP-OVA induce more robust T-cell proliferation than (ζ^-)NP-OVA and soluble OVA alone.

(ζ^+)NP-OVA Up-Regulates BMDC Costimulatory Receptors, Cytokines, and Chemokines. The ability of BMDCs treated with cationic NPs to induce strong OTII T-cell proliferation with ∼100-fold lower concentrations of soluble OVA could be explained by multiple mechanisms. One explanation is that cationic NPs bind more readily to the BMDC surface, resulting in increased antigen uptake and presentation compared with anionic NP or soluble OVA. We tested this possibility by incorporating a pH-sensitive dye (pHrodo) during NP fabrication that fluoresces upon internalization in the endosome. The largest observed difference in NP uptake occurred at 24 h with 20% fewer pHrodo$^+$ cells in (ζ^-)NP-OVA–treated BMDC cultures compared with (ζ^+)NP-OVA treatment (Fig. S2). By 72 h, ≥94% of DCs were pHrodo$^+$ regardless of NP charge (Fig. S2), suggesting that internalization at longer time points is not grossly different between (ζ^+)NP-OVA and (ζ^-)NP-OVA.

We also hypothesized that (ζ^+)NP-OVA–treated DCs induce stronger T-cell proliferation due to increased MHCII and CD80/CD86 expression on the DC surface, which would allow for stronger T-cell receptor engagement and more robust T-cell activation. Flow cytometric analysis indicated that surface MHCII, CD80, and CD86 were up-regulated at 72 h after (ζ^+)NP-OVA treatment, which were similar to the expression

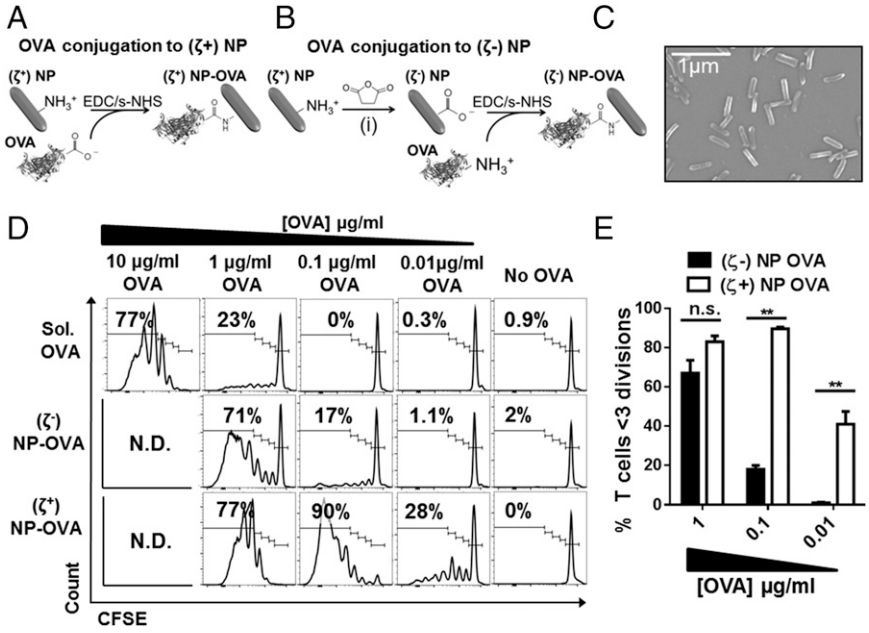

Fig. 1. CD4$^+$ OT-II T-cell proliferation in response to BMDCs treated with ovalbumin functionalized PRINT particles. (*A*) Model antigen OVA was covalently linked to cationic (ζ^+) monodisperse PRINT 80 × 80 × 320 nm particles by using EDC/s-NHS carbodiimide chemistry yielding (ζ^+)NP-OVA. (*B*) Amine groups in (ζ^+)NP were converted to carboxylic groups by using succinic anhydride (i) to yield anionic (ζ^-)NP that were covalently linked to OVA by using the same chemistry as in *A*. (*C*) Representative scanning EM micrograph of functionalized NPs. (*D*) Representative CFSE dilution plots of OVA-specific CD4$^+$VB5.1$^+$ OT-II T-cell division after 72 h coculture with BMDC treated with equivalent does of OVA protein. Soluble OVA (*Upper*), (ζ^-) NP-OVA (*Middle*), and (ζ^+) NP-OVA (*Lower*). Number represents frequency of OVA-specific CD4$^+$ T cells that underwent >3 divisions. N.D., not done. (*E*) Combined data from three experiments described in *A* by using independently synthesized NP-OVA batches. $^{**}P < 0.001$ two-way ANOVA with Sidak's multiple comparisons test. Data graphed as mean ± SEM.

levels observed on LPS-treated DCs after 24 h (Fig. 2*A*). In contrast, (ζ^-)NP-OVA only induced a modest increase in MHCII and coreceptor expression compared with untreated controls (Fig. 2*A*). Maximal levels of MHCII and coreceptor expression induced by (ζ^+)NP-OVA depended on direct OVA conjugation to the NP surface, because blank (ζ^+)NP alone, or (ζ^+)NP administered with soluble OVA [(ζ^+)NP + sol. OVA], were unable to induce strong surface expression of these molecules (Fig. 2*A*). The increase in coreceptor expression was not due to general up-regulation of cell surface molecules, because CD11b expression remained constant among all treatment groups (Fig. 2*A*). Similar results were observed at the mRNA level by using quantitative RT-PCR (qRT-PCR) for CD80 and CD86 at 24 and 48 h after NP treatment (Fig. S3 and Fig. 2*B*, respectively); however, the mRNA levels of *H2-Aa* (MHCII encoding) remained unchanged, suggesting that up-regulation of surface MHCII occurs posttranscriptionally.

We further tested whether BMDC cytokine profiles changed following NP treatment and whether NP charge was a contributing factor. We found significant increases in IL-6 and IL-12 mRNA expression and protein secretion by DCs treated with (ζ^+)NP-OVA compared with (ζ^-)NP-OVA treatment and untreated controls (Fig. S4 *A* and *B*). Increases in key cytokines/chemokines, including *Il1b, Il18*, *Cxcl10*, *Il10*, and *Ifnb*, were detected after DC treatment with (ζ^+)NP-OVA, compared with untreated or (ζ^-)NP-OVA–treated DCs (Fig. S4*A*). Significant increases in *Il18* and *Cxcl10* were observed in DCs treated with (ζ^-)NP-OVA compared with untreated controls; however, at a lower level than (ζ^+)NP-OVA (Fig. S4*A*). Although *Il1b* mRNA expression was elevated in (ζ^+)NP-OVA–treated DCs compared with untreated controls (Fig. S4*A*), we failed to detect IL-1β protein in the supernatant, which is consistent with previous findings that this formulation of NPs does not induce inflammasome activation (18). We also assessed the mRNA expression of several other cytokines (*Ccl2*, *Tnf*, *Tgfb1*, *Il4*) and found that they were either not expressed or were no different from untreated cells (Fig. S4*A*). Similar to T-cell coreceptor expression, the increased cytokine expression/secretion required direct OVA conjugation to the NP, because blank NPs and blank NPs + soluble OVA did not induce strong cytokine responses (Fig. S4 *A* and *B*). These data suggest that cationic NPs induce an activated DC phenotype that requires direct conjugation of protein antigen to the NP surface.

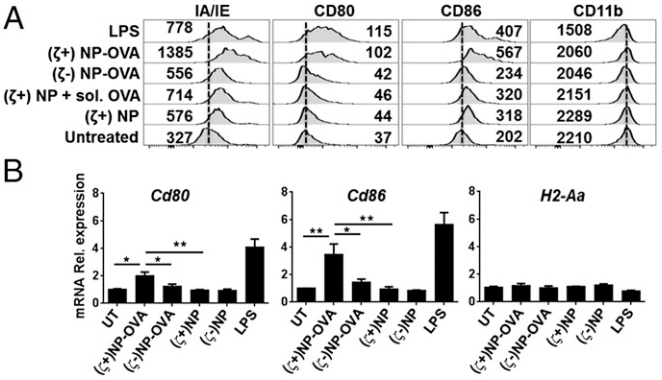

Fig. 2. MHCII and T-cell coreceptor expression by BMDC following NP-OVA treatment. (*A*) Flow cytometric analysis of surface MHCII (IA/IE), CD80, CD86, and CD11b (control) expression on $CD11b^+CD11c^+$ gated BMDCs 48 h after NP treatment. Dashed line indicates average expression level on untreated cells (UT); number indicates MFI. (*B*) qRT-PCR for mRNA expression of *Cd80 Cd86* and *H2-Aa* (MHCII) by cells treated for 48 h as in *A*. Data are normalized to β-actin (*Actb*) mRNA and graphed as fold change over UT. Equivalent OVA dose [1 μg/mL] corresponds to [10 μg/mL] NP dose: LPS treatment for 24 h at 10 ng/mL. $*P < 0.05$, $**P < 0.001$; LPS group was excluded from statistical analysis. Representative of three independent experiments. Each experiment used independently synthesized NP and NP-OVA batches. Bar represents mean ± SEM.

(ζ^+)NP-OVA Have in Vivo Adjuvant Effects Following Pulmonary Immunization. It is well established that effective antibody responses to protein antigens require helper $CD4^+$ T cells. In the absence of T-cell help, the processes of affinity maturation (enhancement of antibody specificity) and Ig isotype switch (IgM to other effector isotypes; IgG, IgA, or IgE) are severely hindered (5). Affinity maturation and isotype switch occur within GCs of dLNs and are comprised of proliferating B cells that up-regulate the surface marker GL7. We used a model of orotracheal NP lung instillation to assess primary and secondary $CD4^+$ T-cell–dependent immune responses, including GC formation and Ig isotype switch by using the immunization schedule described in Fig. S5*A*. We tested whether particulate OVA induces GC formation in the local lung draining medistinal LNs following primary and secondary lung instillations and found significantly higher induction of $CD19^+GL7^+$ GC B cells in (ζ^+)NP-OVA–treated mice compared with (ζ^-)NP-OVA or soluble OVA alone (Fig. 3 *A* and *B*, full gating in Fig. S5*B*). Increased GC B-cell populations in (ζ^+)NP-OVA–treated mice were similar to those treated with soluble CpG/OVA (Fig. 3 *A* and *B*) and were confined to the draining mediastinal LN and not observed in the spleen (Fig. S5*C*), suggesting that induction of GC B cells was due to localized adjuvant activity in the lung and not due to systemic increases in GC B-cell populations in these mice. We also investigated the activation status of $CD4^+$ T cells in the mediastinal lymph node after the secondary instillation and found a significant increase in the frequency of antigen-experienced $CD4^+CD44^{hi}CD62^{lo}$ T cells in (ζ^+)NP-OVA and soluble OVA/CpG-instilled mice compared with mice-treated soluble OVA alone (Fig. 3*C*, gating in Fig. S6*A*). In contrast, the antigen-experienced $CD4^+$ T-cell population was not increased in (ζ^-)NP-OVA–treated mice compared with soluble OVA alone (Fig. 3*C*) and we found no difference in the $CD4^+$ $CD44^{hi}CD62^{lo}$ T-cell populations in spleen (Fig. S6*B*), suggesting that the increase in T effector memory cells is specific to the dLN.

Consistent with increased GC formation and antigen-experienced $CD4^+$ T-cell populations, we readily detected OVA-specific IgG in the plasma and bronchoalveolar lavage fluid (BALF) of (ζ^+)NP-OVA–treated mice following primary and secondary immunization, with titers comparable to those treated with soluble OVA/CpG (Fig. 4 *A* and *B*). Mice treated with (ζ^-)NP-OVA had very low OVA-specific plasma and BALF IgG antibody titers that were not statistically different from mice treated with soluble OVA alone (Fig. 4 *A* and *B*). Three of six mice treated with (ζ^+)NP-OVA had detectable levels of OVA-specific IgA in BALF following primary immunization, whereas no antigen-specific IgA was detected in any other group, including soluble OVA/CpG (Fig. 4*C, Left*). OVA-specific BALF IgA was only detectable in (ζ^+)NP-OVA and soluble OVA/CpG–treated mice following secondary immunization (Fig. 4*C, Right*), indicating that (ζ^+)NP-OVA has an adjuvant effect capable of inducing systemic and mucosal antibody responses similar to the TLR ligand CpG, with no IgA produced in response to (ζ^-)NP-OVA. To determine whether the adjuvant effect(s) of (ζ^+)NP-OVA work through a common mechanism to CpG, we codelivered soluble CpG with (ζ^+)NP-OVA to test for additive effects on OVA-specific antibody titers. We observed that codelivery of soluble CpG with (ζ^+)NP-OVA significantly increased levels of OVA-specific BALF IgG and IgA compared with soluble OVA/CpG (Fig. 4*D*), suggesting that (ζ^+)NP-OVA and CpG work in an additive fashion to induce more robust antibody responses, especially for mucosal IgA (Fig. 4*D, Right*). We also observed that codelivery of soluble CpG rescued the ability of (ζ^-)NP-OVA to induce BALF IgG and IgA responses (Fig. 4*D*), suggesting that anionic NPs can still serve as a platform for antigen delivery, but antibody responses require coupling to TLR

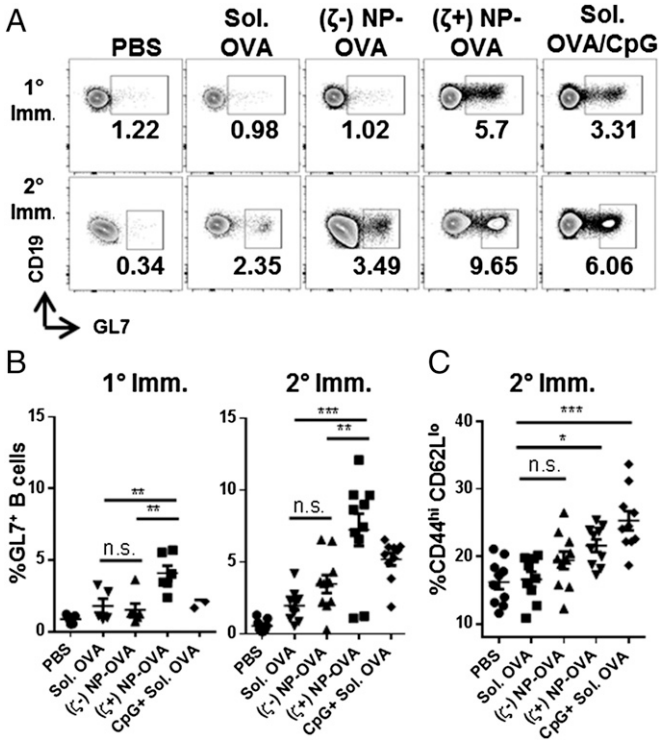

Fig. 3. GC B-cell formation and $CD4^+$ T-cell activation in mediastinal LNs following pulmonary immunization. (*A*) Representative flow plots for frequency of $CD19^+GL7^+$ GC B cells in the mediastinal LN following 1° and 2° immunization. (*B*) Combined data from *A*; 1° immunization, ($n \geq 5$) per group; 2° immunization, $n \geq 10$ per group. (*C*) Frequency of antigen-experienced $CD4^+CD44^{hi}CD62L^{lo}$ T cells in mediastinal LN after 2° immunization ($n \geq 10$ per group). $^*P < 0.05$, $^{**}P < 0.01$, $^{***}P < 0.001$, n.s., not significant; one-way ANOVA with Tukey's multiple comparisons test. Data in *A* are representative of two independent experiments. Data in *B* and *C* are combined from two independent experiments. Each experiment used independently synthesized NP and NP-OVA batches. NP dose = 100 μg per instillation (10 μg of OVA); CpG dose = 2.5 μg per instillation. Line represents mean ± SEM.

agonists. From these data, we conclude that cationic NPs contain inherent adjuvant activity that can further synergize with TLR-stimulating adjuvants, such as CpG, when delivered to the lung.

The in Vivo Adjuvant Effect(s) of (ζ^+)NP-OVA Are Independent of Endotoxin Contamination. Certain sources of purified OVA contain endotoxin contaminants that can confound the results of immunization studies. The OVA used thus far in this manuscript is grade V from Sigma, which has the highest protein purity, but has also been found in the past (and reported here; Fig. S7), to contain detectable amounts of endotoxin (19). To test whether the adjuvant effect(s) we observe in vivo are independent of OVA-associated endotoxin, we repeated the in vivo immunization studies by using NPs conjugated to vaccine grade endotoxin-free (ef) OVA (Ovalbumin EndoFit; Invivogen, endotoxin levels in Fig. S7). We found that (ζ^+)NP-efOVA still induced OVA-specific IgG responses in plasma and BALF following primary immunization, whereas (ζ^-)NP-efOVA and soluble efOVA failed to induce any detectable antigen-specific Ig (Fig. 5*A*). Following secondary immunization, the antigen-specific IgG in plasma and BALF increased in (ζ^+)NP-efOVA–treated animals, but remained undetectable with (ζ^-)NP-efOVA and soluble efOVA treatment, despite the boost dose (Fig. 5*B*). Additionally, OVA-specific IgA was exclusively detected in BALF of (ζ^+)NP-efOVA–boosted mice and could not be induced even when soluble efOVA was codelivered with the FDA approved TLR4 agonist, Monophosphoryl Lipid A (MPLA) (Fig. 5*B*). Consistent with increased OVA specific antibody responses, we also observed expansion of $CD19^+GL7^+$ GC B cells in the dLN of (ζ^+)NP-efOVA–treated mice compared with (ζ^-)NP-efOVA and soluble efOVA (Fig. S8 *A* and *B*). Our studies using efOVA indicate that cationic NPs exhibit inherent adjuvant properties in the lung that induce GC B-cell expansion, as well as mucosal and systemic antibody production that are independent of endotoxin activity.

Discussion

NP design features, such as size, shape, modulus, and surface chemistry, are well established for long circulating i.v. delivery; however, these parameters are mainly unverified for other routes of administration, especially pulmonary delivery. Our studies used the PRINT fabrication process to isolate surface charge as the sole variable in NP-based pulmonary vaccines, while maintaining identical particle composition, size, shape, and antigen loading. Our results indicate that cationic hydrogel NPs have adjuvant-like effects, yielding potent mucosal and systemic antibody responses following pulmonary delivery, whereas anionic NPs fail to do so. These responses appear T-cell–dependent, because they correlate with increased GC formation and Ig class switch recombination, which are known to require T-cell help (20, 21).

Possible Mechanisms for Enhanced Mucosal and Systemic Antibody Responses by Cationic NPs. The precise mechanism(s) for how antigen-conjugated cationic NPs induce mucosal and systemic antibody responses require further investigation. Previous vaccine-related studies using cationic liposomes showed increased antibody responses over soluble controls; however, this response was solely attributed to enhanced NP binding to the APC surface and no differences in costimulatory molecule or cytokine expression were reported (22–24). We observed that cationic NPs bound more readily to DCs and macrophages in vitro compared with anionic NPs; however, the degree of NP internalization was not grossly different between these groups, especially at longer time points. Building on previous efforts from our laboratory, which established that pulmonary delivery of PRINT NPs do not trigger any lung inflammatory responses by cytokine release or histopathology (18), neither cationic nor anionic NPs triggered local lung or systemic increases in the inflammatory cytokines IL-6, TNF-α, or IL-1β compared with PBS controls. Rather, our finding that T-cell–activating coreceptors and cytokines are induced with cationic NPs, but not with anionic NPs, suggests a clear role of NP charge in DC maturation and effector function. Similar studies using positively charged chitosan-based NPs have also shown enhanced immune responses over whole protein controls (15, 25, 26), and recent cationic NP studies using the macrophage cell line RAW 264.7 have also demonstrated up-regulation of T-cell costimulatory molecules and cytokines (27). Interestingly, our studies suggest that the positive charge alone is insufficient for DC maturation, because this process required protein conjugation to the NP surface. Therefore, the protein antigen in combination with select NP characteristics (e.g., positive charge) may be required for microbial mimicry effects that trigger DC maturation.

The expansion of GC B cells and antigen-experienced $CD4^+$ T cells following cationic NP delivery were confined to the lung dLN, suggesting that these responses use lung resident immune populations. Previous studies established that similar-sized NP (~200 nm) required lung resident DC transport to the dLN for induction of potent $CD4^+$ T-cell responses (28, 29). Based on these studies and our data reported here, we hypothesize that enhanced antibody responses emanate from cationic NP interaction with lung resident DCs that then migrate to the dLN to induce T-cell–dependent GC formation and antibody production. Treatment of DCs with (ζ^+)NP-OVA ex vivo-induced T_H1 skewing cytokine production (IL-12, IL-18), but not T_H2 skewing cytokines (IL-4), suggesting that cationic NPs may instruct T_H cell

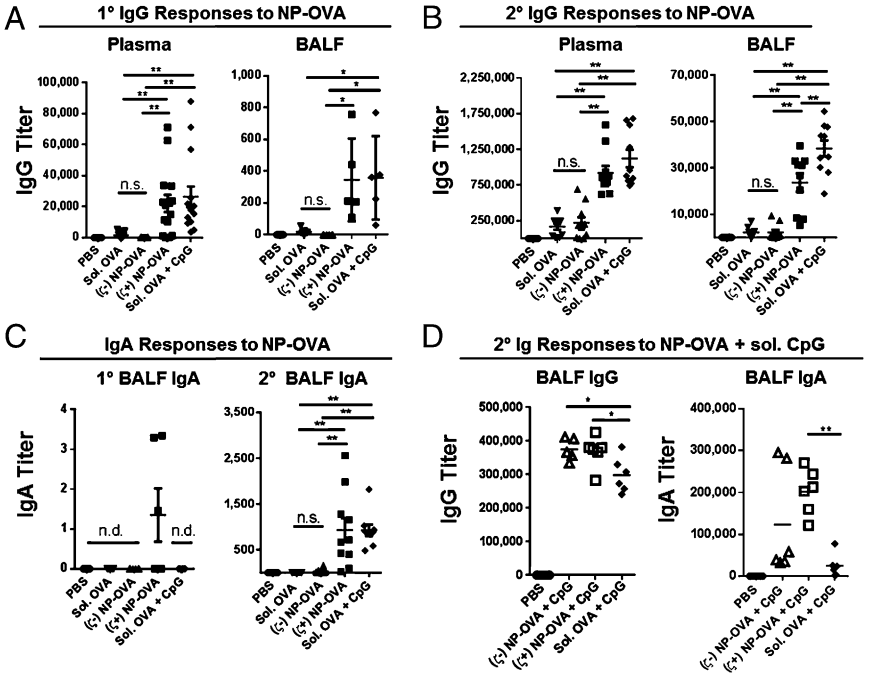

Fig. 4. OVA-specific antibody titers in plasma and BALF of mice following pulmonary immunization with NP-OVA. (*A–D*) ELISA for OVA-specific IgG and IgA. (*A*) Plasma IgG ($n \geq 15$), BALF IgG ($n \geq 5$) following 1° immunization. (*B*) Plasma IgG, BALF IgG ($n \geq 10$) following 2° immunization. (*C*) BALF IgA levels following 1° ($n \geq 5$) and 2° immunization ($n \geq 10$). (*D*) BALF IgG and IgA levels following 2° NP-OVA + soluble CpG ($n \geq 6$). $^*P < 0.05$, $^{**}P < 0.001$; one-way ANOVA with Tukey's multiple comparisons test. Plasma data in *A* are combined from three independent experiments, BALF data in *A* are representative of two independent experiments. BALF data in *B* are combined from two independent experiments. Data in *C* and *D* are representative of two independent experiments. Samples from combined experiments were analyzed simultaneously by ELISA; each experiment used independently synthesized NP and NP-OVA batches. NP dose = 100 μg per instillation (10 μg of OVA); CpG dose = 2.5 μg per instillation. Line represents mean ± SEM.

differentiation. Additionally, increased antibody responses in vivo may result from enhanced activation of specialized T-follicular helper cells, which have been shown to be critical for robust GC formation and antibody production (4). More in-depth studies of how NP charge affects lung DCs and $CD4^+$ T-cell effector populations are needed and are underway.

Synergistic Effects of Cationic NPs and TLR Ligands. Vaccine-grade OVA coupled to cationic NPs was sufficient to induce robust GC B-cell expansion and OVA-specific antibody production in vivo, especially IgA, suggesting that cationic charge confers an adjuvant-like effect that is independent or additive of TLR activity. Cationic particles have been shown to bind anionic macromolecules, such as self-DNA, which may result in low levels of TLR-9 signaling (30, 31). However, use of conventional OVA preparations containing endotoxin, or the exogenous addition of soluble CpG, enhanced the capacity of cationic NPs to induce mucosal and systemic antibody responses by two- to sixfold, indicating that controlled addition of TLR ligands to cationic NPs is a viable option for future pulmonary subunit vaccine development. Perhaps the most surprising finding from our study was that anionic NPs failed to enhance GC formation and antibody responses following pulmonary delivery. Our ex vivo data indicated that DCs treated with (ζ^-)NP-OVA induced stronger OT-II T-cell proliferation compared with soluble OVA, and we expected to see a similar trend in our in vivo studies; however, the response to (ζ^-)NP-OVA was no different from soluble OVA alone. The failure of anionic NPs to induce immune responses was even more apparent when using vaccine grade OVA, which did not induce any detectable OVA-specific antibody. We were able to restore antibody responses to (ζ^-)NP-OVA by coadministering soluble CpG, suggesting that the OVA conjugated to anionic NPs was still intact, but that the negative charge lacks the adjuvant effect associated with cationic NPs.

NP Charge as a Critical Design Parameter for Pulmonary Therapeutics. Our study indicates that consideration of NP charge may be of critical importance when designing pulmonary therapeutics. We have demonstrated that cationic NP formulations delivered to the lung enhance both systemic and mucosal antibody responses while also providing an adjuvant effect, whereas anionic NPs do not. However, the use of anionic particles could be advantageous in cases where immune responses are contraindicated. For example, anionic charge with particulate drug depots may afford stealth-like properties allowing for reduced particle clearance and sustained therapeutic delivery. Studies by other groups show that anionic NPs delivered to the lung can induce potent cell-based immunity by activating $CD8^+$ T-cell responses (16, 17). Together, these studies suggest that the ability to control NP

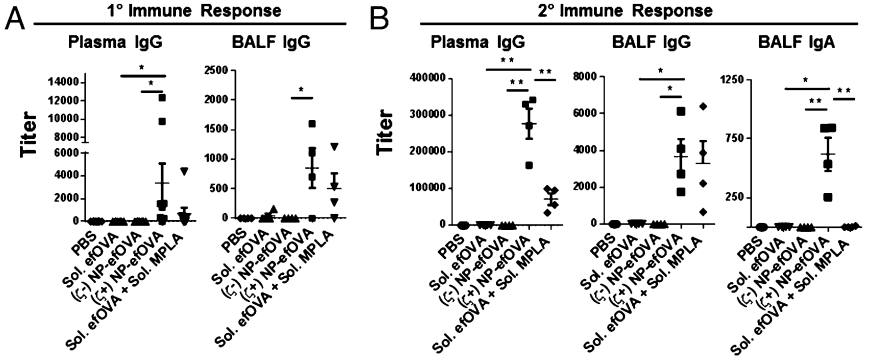

Fig. 5. OVA-specific antibody titers in plasma and BALF of mice following pulmonary immunization with endotoxin-free OVA-conjugated NP (NP-efOVA). ELISA for OVA-specific IgG and IgA. (*A*) Plasma IgG ($n = 8$), BALF IgG ($n = 4$) levels following 1° immunization. (*B*) Plasma IgG ($n = 4$), BALF IgG ($n = 4$), and BALF IgA ($n = 4$) levels following 2° immunization. $^*P < 0.05$, $^{**}P < 0.001$; 1-way ANOVA with Tukey's multiple comparisons test. NP dose = 100 μg per instillation (10 μg of OVA); MPLA dose = 0.3 μg per instillation. Line represents mean ± SEM.

surface charge offers opportunities to tailor the therapeutic application based on desired immunological response.

Continuing to investigate and understand how surface charge and other particle parameters affect cellular interaction/biological responses will be critical for engineering novel NP therapeutics. The degree of control and NP scalability afforded by PRINT allows for intricate vaccine design with the capacity to alter NP dimensions, use cleavable linkers for antigen/adjuvant conjugation, and aerosol formulation to provide a portable pulmonary route of administration (18, 32). Our findings will hopefully contribute to future development of pulmonary-based vaccine platforms that are applicable to a diverse array of pathogens.

Materials and Methods

Particle Fabrication. Amine-containing 80 × 320 nm hydrogel rod-shaped NPs were fabricated on a continuous roll-to-roll PRINT method as described (33). Preparticle solutions contained 1% diphenyl(2,4,6-trimethylbenzoyl)phosphine oxide, 20% (wt/wt) 2-aminoethyl methacrylate hydrochloride, 10% (wt/wt) poly (ethylene glycol) diacrylate (Mn~700), 0–1% functional fluorescent dye, and 69–68% (wt/wt) tetra(ethylene glycol) monoacrylate. OVA functionalization was achieved by using carbodiimide chemistry. Characterization of NPs is described in *SI Materials and Methods*.

OT-II Coculture. Cell preparation and additional analysis are described in *SI Materials and Methods*. On day 0, BMDCs were seeded in RPMI 1640 with glutamine (Gibco) and 10% (vol/vol) FBS in a round-bottom 96-well plate. NPs or soluble OVA were added on day 1 based on mass of OVA per well. On day 2, splenocytes from OT-II mice were harvested and purified. $CD4^+$ OT-II T cells were labeled by using CellTrace Violet (CFSE analog, referred to in the text as CFSE) following manufacturer's protocol (Life Technologies). T cells were added to NP-treated BMDCs. Cells were harvested 72 h after T-cell addition.

Pulmonary Delivery and Immunizations. All studies were conducted in accordance with National Institutes of Health guidelines for the care and use of laboratory animals and approved by the Institutional Animal Care and Use Committee at the University of North Carolina (UNC). All animals were maintained in pathogen-free facilities at UNC and were between 8 and 15 wk of age. C57BL/6 mice were obtained from Jackson Laboratories and OT-II transgenic mice were bred in-house. NP and control formulations were delivered to the lungs of anesthetized mice through an orotracheal instillation in a 50-μL volume. NP doses were 100 μg of NP per instillation, corresponding to 10 μg of OVA per instillation, which was used as the control soluble OVA dose; in studies with adjuvant, 2.5 μg of CpG per instillation or 0.3 μg of MPLA per instillation was also delivered. For single-dose immunization studies, a dose was give on day 0 and euthanasia performed on day 9. For prime and boost immunization studies, doses were given on day 0 and 10, with submandibular bleeds performed on day 9 and euthanasia on day 20. Characterization of tissue preparation, antibody responses, GC formation, and T-cell activation is described in *SI Materials and Methods*.

Statistical Analysis. Statistical analyses were performed with GraphPad Prism version 6. Analysis of groups was performed as indicated in figures. All data points were included in the analyses, and no outliers were excluded in calculations of means or statistical significance.

ACKNOWLEDGMENTS. We thank R. Roberts, C. Luft, T. Rahhal, K. Reuter, J. Perry, C. Kapadia, S. Tian, A. Pandya, N. Fisher, and S. Coquery for useful discussions and technical assistance. We acknowledge Liquidia Technologies for providing PRINT molds. We thank the University of North Carolina (UNC) Flow Cytometry Core (Grant P30CA016086), Chapel Hill Analytical and Nanofabrication Laboratory (CHANL), and UNC Division of Laboratory Animal Medicine (DLAM). This work was funded in part by NIH Pioneer Award 1DP1OD006432 (to J.M.D.), NIH Grant U19AI109784 (to J.P.Y.T. and J.M.D.), and Defense Threat Reduction Agency (DTRA) Award HDTRA1-13-1-0045 (to J.M.D.).

1. Neutra MR, Kozlowski PA (2006) Mucosal vaccines: The promise and the challenge. *Nat Rev Immunol* 6(2):148–158.
2. Blank F, Stumbles P, von Garnier C (2011) Opportunities and challenges of the pulmonary route for vaccination. *Expert Opin Drug Deliv* 8(5):547–563.
3. Borges O, Lebre F, Bento D, Borchard G, Junginger HE (2010) Mucosal vaccines: Recent progress in understanding the natural barriers. *Pharm Res* 27(2):211–223.
4. Qi H, et al. (2014) Follicular T-helper cells: Controlled localization and cellular interactions. *Immunol Cell Biol* 92(1):28–33.
5. Jacobson EB, Caporale LH, Thorbecke GJ (1974) Effect of thymus cell injections on germinal center formation in lymphoid tissues of nude (thymusless) mice. *Cell Immunol* 13(3):416–430.
6. Inaba K, Steinman RM, Van Voorhis WC, Muramatsu S (1983) Dendritic cells are critical accessory cells for thymus-dependent antibody responses in mouse and in man. *Proc Natl Acad Sci USA* 80(19):6041–6045.
7. Rickert RC, Rajewsky K, Roes J (1995) Impairment of T-cell-dependent B-cell responses and B-1 cell development in CD19-deficient mice. *Nature* 376(6538):352–355.
8. Smith DM, Simon JK, Baker JR, Jr (2013) Applications of nanotechnology for immunology. *Nat Rev Immunol* 13(8):592–605.
9. Zhao L, et al. (2014) Nanoparticle vaccines. *Vaccine* 32(3):327–337.
10. Hardy CL, et al. (2013) Differential uptake of nanoparticles and microparticles by pulmonary APC subsets induces discrete immunological imprints. *J Immunol* 191(10):5278–5290.
11. Kunda NK, Somavarapu S, Gordon SB, Hutcheon GA, Saleem IY (2013) Nanocarriers targeting dendritic cells for pulmonary vaccine delivery. *Pharm Res* 30(2):325–341.
12. Pulliam B, Sung JC, Edwards DA (2007) Design of nanoparticle-based dry powder pulmonary vaccines. *Expert Opin Drug Deliv* 4(6):651–663.
13. Wang YY, et al. (2008) Addressing the PEG mucoadhesivity paradox to engineer nanoparticles that "slip" through the human mucus barrier. *Angew Chem Int Ed Engl* 47(50):9726–9729.
14. Debin A, et al. (2002) Intranasal immunization with recombinant antigens associated with new cationic particles induces strong mucosal as well as systemic antibody and CTL responses. *Vaccine* 20(21-22):2752–2763.
15. Gupta NK, Tomar P, Sharma V, Dixit VK (2011) Development and characterization of chitosan coated poly-(ε-caprolactone) nanoparticulate system for effective immunization against influenza. *Vaccine* 29(48):9026–9037.
16. Nembrini C, et al. (2011) Nanoparticle conjugation of antigen enhances cytotoxic T-cell responses in pulmonary vaccination. *Proc Natl Acad Sci USA* 108(44):E989–E997.
17. Li AV, et al. (2013) Generation of effector memory T cell-based mucosal and systemic immunity with pulmonary nanoparticle vaccination. *Sci Transl Med* 5(204):ra130.
18. Roberts RA, et al. (2013) Analysis of the murine immune response to pulmonary delivery of precisely fabricated nano- and microscale particles. *PLoS ONE* 8(4):e62115.
19. Watanabe J, Miyazaki Y, Zimmerman GA, Albertine KH, McIntyre TM (2003) Endotoxin contamination of ovalbumin suppresses murine immunologic responses and development of airway hyper-reactivity. *J Biol Chem* 278(43):42361–42368.
20. Good-Jacobson KL, Tarlinton DM (2012) Multiple routes to B-cell memory. *Int Immunol* 24(7):403–408.
21. Parker DC (1993) T cell-dependent B cell activation. *Annu Rev Immunol* 11:331–360.
22. Christensen D, et al. (2009) Liposome-based cationic adjuvant formulations (CAF): Past, present, and future. *J Liposome Res* 19(1):2–11.
23. Korsholm KS, et al. (2007) The adjuvant mechanism of cationic dimethyldioctadecylammonium liposomes. *Immunology* 121(2):216–226.
24. Ma Y, et al. (2011) The role of surface charge density in cationic liposome-promoted dendritic cell maturation and vaccine-induced immune responses. *Nanoscale* 3(5):2307–2314.
25. Slütter B, Jiskoot W (2010) Dual role of CpG as immune modulator and physical crosslinker in ovalbumin loaded N-trimethyl chitosan (TMC) nanoparticles for nasal vaccination. *J Control Release* 148(1):117–121.
26. van der Lubben IM, Verhoef JC, Borchard G, Junginger HE (2001) Chitosan and its derivatives in mucosal drug and vaccine delivery. *Eur J Pharm Sci* 14(3):201–207.
27. Koppolu B, Zaharoff DA (2013) The effect of antigen encapsulation in chitosan particles on uptake, activation and presentation by antigen presenting cells. *Biomaterials* 34(9):2359–2369.
28. Choi HS, et al. (2010) Rapid translocation of nanoparticles from the lung airspaces to the body. *Nat Biotechnol* 28(12):1300–1303.
29. Furuhashi K, et al. (2012) Mouse lung CD103+ and CD11bhigh dendritic cells preferentially induce distinct CD4+ T-cell responses. *Am J Respir Cell Mol Biol* 46(2):165–172.
30. Coch C, et al. (2009) Higher activation of TLR9 in plasmacytoid dendritic cells by microbial DNA compared with self-DNA based on CpG-specific recognition of phosphodiester DNA. *J Leukoc Biol* 86(3):663–670.
31. Gilliet M, Cao W, Liu YJ (2008) Plasmacytoid dendritic cells: Sensing nucleic acids in viral infection and autoimmune diseases. *Nat Rev Immunol* 8(8):594–606.
32. Garcia A, et al. (2012) Microfabricated engineered particle systems for respiratory drug delivery and other pharmaceutical applications. *J Drug Deliv* 2012:941243.
33. Perry JL, et al. (2012) PEGylated PRINT nanoparticles: The impact of PEG density on protein binding, macrophage association, biodistribution, and pharmacokinetics. *Nano Lett* 12(10):5304–5310.